Aggregation of rod-like polyelectrolyte chains in the presence of monovalent counterions

3 AUTHORS, INCLUDING:

R. Rajesh
The Institute of Mathematical Sciences
73 PUBLICATIONS **530** CITATIONS

Satyavani Vemparala
The Institute of Mathematical Sciences
35 PUBLICATIONS **618** CITATIONS

Aggregation of rod-like polyelectrolyte chains in the presence of monovalent counterions

Anoop Varghese,[1, a)] R. Rajesh,[1, b)] and Satyavani Vemparala[1, c)]

The Institute of Mathematical Sciences, C.I.T. Campus, Taramani, Chennai 600113, India

(Dated: 4 December 2012)

Using molecular dynamics simulations, it is demonstrated that monovalent counterions can induce aggregation of similarly charged rod-like polyelectrolyte chains. The critical value of the linear charge density for aggregation is shown to be close to the critical value for the extended–collapsed transition of a single flexible polyelectrolyte chain, and decreases with increasing valency of the counterions. The potential of mean force along the center of mass reaction coordinate between two similarly charged rod-like polyelectrolytes is shown to develop an attractive well for large linear charge densities. In the attractive regime, the the angular distribution of the condensed counterions is no longer isotropic.

I. INTRODUCTION

Polyelectrolytes (PEs) are charged polymers in a solution containing neutralizing counterions[1–3]. They are common in biological systems, examples include DNA[4], F-actin and microtubules[5]. A special case is a rod-like PE (RLPE) whose persistence length is of the order of its contour length. RLPEs are of interest theoretically because their thermodynamics is similar to the theoretically well studied idealized system of a charged cylinder with neutralizing counterions.

PEs, even if similarly charged, may attract each other in the presence of counterions. The aggregation of similarly charged PEs has been extensively studied experimentally[4–13], theoretically[14–25] and numerically[26–35]. Despite these studies, the role of counterion valency in aggregation remains unclear. Though it has been shown unambiguously that multivalent counterions can mediate aggregation[4–9,11–24,26–30,32–35], it is still being debated whether monovalent counterions can cause aggregation in the absence of multivalent salts. There are some experimental[6–10] and theoretical[18,24] results that argue for monovalent counterion induced aggregation of PEs. At the same time, other experimental[11,13], theoretical[17,36,37] and numerical[26–31] studies argue or report the absence of aggregation in the presence of monovalent counterions.

There are different proposals for understanding the attraction between two similarly charged PEs. One of them suggests that the attraction is induced by the correlated longitudinal fluctuations of the condensed counterion density[16]. This theory predicts attraction in the presence of multivalent counterions, in agreement with early numerical simulations[26], for a range of system parameters. The validity of the Gaussian approximation made in the theory was questioned[36,38], and more realistic, but simple models were considered[17,36]. These models assume localization of the condensed counterions on a finite number of allowed sites around the PEs, and were

able to explain multivalent counterion induced attraction in terms of spatial distribution of the condensed counterions around the PEs. However, these theories predict a very weak[17] or zero[38] attraction for the case of monovalent counterions.

An alternate approach that explains the attraction of PEs is by Manning et. al.[18], and is based on the classical condensation theory[39]. Though this approach does not explicitly take into account correlations between counterions, it predicts attraction between similarly charged PEs. In fact, the theory predicts stronger attraction in the presence of monovalent counterions than divalent or trivalent counterions. The origin of attraction is similar to that of covalent bonds, in that the condensed counterions are shared by the PEs. This theory was later extended[23,24], using extended condensation theory[40], to calculate the interaction free energy as a function of the separation between the PEs, linear charge density of the PEs and valency of the counterions. The analysis of the free energy shows that the attraction is a consequence of the increase in the number of condensed counterions and the counterion condensation volume with decrease in the separation between the PEs. This approach differs from the Manning theory in that the assumption of infinite dilution of added salt is absent. Although these theories predict the formation of stable aggregates, mediated by monovalent counterions, a clear experimental or computational confirmation is still lacking. Most earlier numerical simulations[26–31,34] do not observe attraction that is strong enough to form stable aggregates.

A different phenomena in PE systems, mediated by counterions, is the extended–collapsed transition of a single flexible[41–46] or semi-flexible PE[47]. As the linear charge density exceeds a critical value, an extended flexible PE chain undergoes a first-order transition[42,44] to a globular phase, while an extended semi-flexible PE transforms into a toroid-like phase[47]. As for aggregation of PEs, there are different proposals for the underlying mechanism of the extended–collapsed transition. In one of the approaches, a one-component plasma model of the PE system was shown to have negative compressibility when the linear charge density of the PE chain exceeds a critical value[42]. The negative compressibility causes

a)Electronic mail: anoop@imsc.res.in
b)Electronic mail: rrajesh@imsc.res.in
c)Electronic mail: vani@imsc.res.in

the PE chain to collapse, with the transition being first-order. In an alternate approach[43], the transition was studied using a two-state model, where the free energy of the extended and collapsed phases of PE chain was calculated. The collapsed phase was approximated by an amorphous ionic solid made up of the condensed counterions and the monomers of the PE chain, and the strong correlation between the counterions and the monomers was argued to be responsible for the collapse of the chain. In an another numerical study[41], the condensed counterions were shown to form dipoles with the monomers of the chain, and the resultant dipole-dipole attraction causes the chain to collapse. A different approach[47], based on the dependence of the free energy of a semi-flexible PE chain on counterion density fluctuations, argued that the extended phase of a semi-flexible PE chain destabilizes into a toroid-like phase at high linear charge densities.

In this paper, using molecular dynamics simulations (details in Sec. II), we demonstrate the aggregation of similarly charged RLPEs in the presence of monovalent counterions when the linear charge density of the polymer backbone is higher than a critical value (Sec. III A). We argue that the critical backbone charge densities required for the onset of aggregation of RLPEs and the extended–collapsed transition of a single flexible PE chain are nearly equal (Sec. III B). We also measure the potential of mean force between two RLPEs along the distance between their centers of mass and show the existence of an attractive well for large linear charge densities (Sec. III C). In this attractive regime, a spatial rearrangement of counterions around a RLPE occurs and is quantified in Sec. III D. Sec. IV contains a summary and discussion.

II. MODEL AND SIMULATION METHOD

We model RLPE and flexible PE chains as N spheres (monomers), each with charge $+qe$, connected through springs. The counterions are modelled as spheres with charge $-Zqe$, where $Z = 1, 2$ and 3 for monovalent, divalent and trivalent counterions respectively. All counterions have same valency, and the number of counterions is such that the system is overall charge neutral. The polymer chain and the counterions are assumed to be in a medium of uniform dielectric constant ϵ.

The interactions between particles i and j are of four types:

Coulomb interaction: The electrostatic energy is given by

$$U_c(r_{ij}) = \frac{q_i q_j}{4\pi\epsilon\epsilon_0 r_{ij}}, \qquad (1)$$

where r_{ij} is the distance between particle i and j, and q_i is the charge of the ith particle, and ϵ_0 is the permittivity of free space.

Excluded volume interaction: The excluded volume interactions are modelled by the Lennard-Jones potential,

which for two particles at a distance r_{ij}, is given by

$$U_{LJ}(r_{ij}) = 4\epsilon_{ij} \left[\left(\frac{\sigma}{r_{ij}} \right)^{12} - \left(\frac{\sigma}{r_{ij}} \right)^{6} \right], \qquad (2)$$

where ϵ_{ij} is the minimum of the potential and σ is the inter-particle distance at which the potential becomes zero. We use reduced units, in which the energy and length scales are specified in units of ϵ_{ij} and σ respectively. The depth of the attractive potential ϵ_{ij} and its range σ are set to 1.0 for all pairs of particles. We use shifted Lennard-Jones potential in which $U_{LJ}(r_{ij})$ smoothly goes to zero beyond a cut off distance r_c. The value of r_c is chosen to be 1.0 such that the excluded volume interaction is purely repulsive for all pairs, mimicking polymers in good solvents.

Bond stretching interaction: The bond stretching energy for pairs that are connected through springs is given by

$$U_b(r_{ij}) = \frac{1}{2} k_b (r_{ij} - b)^2, \qquad (3)$$

where k_b is the spring constant and b is the equilibrium bond length. The values of k_b and b are taken as 500 and 1.12 respectively. This value of b is close to the minimum of Lennard-Jones potential, and the spring constant k_b is large enough so that the bond length does not change appreciably from b.

Bond bending interaction: The rigidity of the polymer backbone is controlled by a three-body interaction given by

$$U_\theta(\theta) = k_\theta [1 + \cos\theta], \qquad (4)$$

where θ is the angle between two adjacent bonds. For RLPEs, we choose $k_\theta = 10^3$ to ensure rigidity of the backbone, while k_θ is set to zero for flexible PEs.

The relative strength of the electrostatic interaction is parameterized by a dimensionless quantity A:

$$A = \frac{q^2 \ell_B}{b}, \qquad (5)$$

where ℓ_B is the Bjerrum length[48],

$$\ell_B = \frac{e^2}{4\pi\epsilon\epsilon_0 k_B T}, \qquad (6)$$

where k_B is the Boltzmann constant and T is temperature. In our simulations, we vary A from 0.22 to 10.93.

The equations of motion are integrated in time using the molecular dynamics simulation package LAMMPS[49,50]. The simulations are carried out at constant temperature (T=1.0), maintained through a Nosé-Hoover thermostat (coupling constant = 0.1)[51,52]. The system is placed in a cubic box with periodic boundary conditions. We use the particle-particle/particle-mesh (PPPM) technique[53] to evaluate the energy and forces due to the long range Coulomb interactions. The time

step for the integration of the equations of motion is chosen as 0.001.

In the current study, three systems are considered. In the first system, aggregation of 50 similarly charged RLPEs with varying linear charge densities neutralized by counterions of varying valency is studied. In the second set of simulations, we locate the extended–collapsed transition point of a single flexible PE chain in the presence of counterions of different valency. In the third set of simulations, we measure the potential of mean force between two RLPEs in the presence of monovalent counterions to understand the observed aggregation.

III. RESULTS AND DISCUSSION

A. Aggregation of rod-like polyelectrolyte chains

To study aggregation, we consider a collection of 50 RLPE chains of 30 monomers each. The system is charge neutralized with monovalent, divalent or trivalent counterions. The density of the system is chosen to be 4.4×10^{-4} monomers/σ^3. At this density, the mean separation between the chains is much larger than the length of the chains. We vary the non-dimensional parameter A from 0.22 to 10.93.

We first show that monovalent counterions can mediate aggregation of similarly charged RLPEs, in contrast to the previous experimental[11,13], theoretical[17,36,37] and numerical[26–31] studies. In Fig. 1(A)–(D), we show snap shots of the system at increasing times for $A = 9.43$, when all counterions are monovalent. For this value of A, electrostatic interactions are much larger than thermal energies, and aggregation of RLPEs can clearly be seen.

We quantify aggregation by calculating the dependence of average aggregate size on A. Two PE chains are defined to form an aggregate if the distance between any monomer of the first chain and any monomer of the second chain is less than 2σ. Similarly, a PE chain is defined to be part of an aggregate of size m $(m > 2)$ if the distance between any of its monomers and any monomer of the other $m-1$ chains is less than 2σ. Other similar definitions for what constitutes an aggregate can be found in the literature[27,32,35], but we find that the results do not change noticeably with different choices of the definition.

Let N_m be the number of aggregates of size m. Then, the average aggregate size is given by $\sum_{m=1}^{50} m N_m / \sum_{m=1}^{50} N_m$. Measuring the equilibrium value of N_m turns out to be difficult in the aggregate regime because of large equilibration times and limited computational time. We, therefore, measure N_m after starting from two different types of initial conditions and discarding a fixed number of initial simulation steps. In the first type, we start from an initial random configuration of RLPEs and discard the first 3×10^7 time steps. We then average the aggregate size over the next 10^7
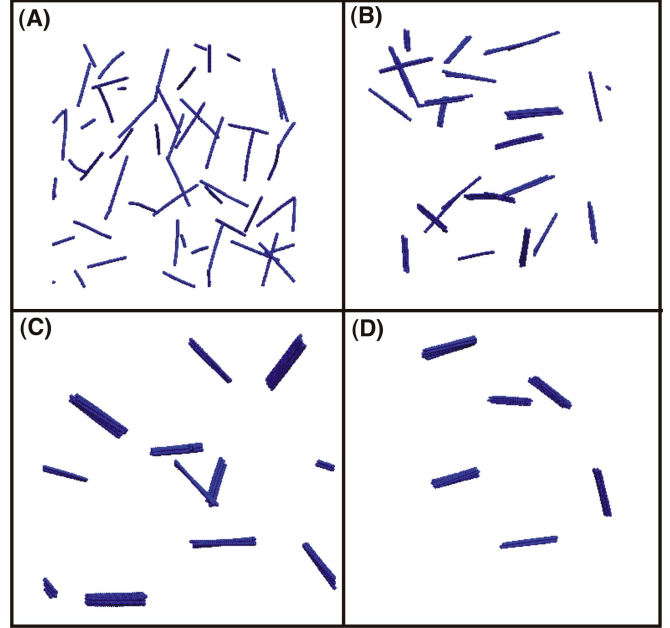

FIG. 1. The two dimensional projection of the RLPEs at time steps (A) 0, (B) 1.90×10^6, (C) 8.90×10^6 and (D) 4.72×10^7. The counterions are monovalent and are not shown for clarity. The RLPEs aggregate, with the number of aggregates decreasing in time. The data are for $A = 9.43$.

time steps. The average aggregate size, thus computed, is shown by crosses in Fig. 2(A) as a function of A for counterions of different valency. The aggregation begins at critical values $A = 6.57, 2.50$ and 1.45 for monovalent, divalent and trivalent counterions respectively, which correspond to an average aggregate size of 2.0. At high enough values of A, all the 50 chains form a single aggregate for both divalent and trivalent counterions. However, in the case of monovalent counterions, even for the highest value of A (10.93) that we studied, we did not observe formation of a single aggregate within the maximum duration of our simulations (5×10^7), and the final configuration of the system consists three aggregates of approximately 16 PEs each. In the second set of simulations, we start with a high value of A and an initial condition where all the chains are in an aggregate. We then discard the first 10^7 time steps, and measure the aggregate size over the next 10^6 time steps. A is then decreased and the initial condition is chosen to be final state of the previous A value. The data thus obtained are shown by circles in Fig. 2(A). The values for A for which the two kinds of runs give the same value for average aggregate size can be taken to be the correct equilibrium value. The formation of a hysteresis loop is clearly seen.

The difficulty in equilibration in the aggregating regime is due to large diffusion time scales. As small aggregates form, they take longer and longer to diffuse and come close to each other before the next aggregation event can occur. We find that for values of A larger than

FIG. 3. The variation of $\langle N_a \rangle$, the average number of aggregates, with time t for different values of A and valency. The data is log-binned and averaged over five different initial configurations. The solid black line is a power law $\sim t^{-2/3}$
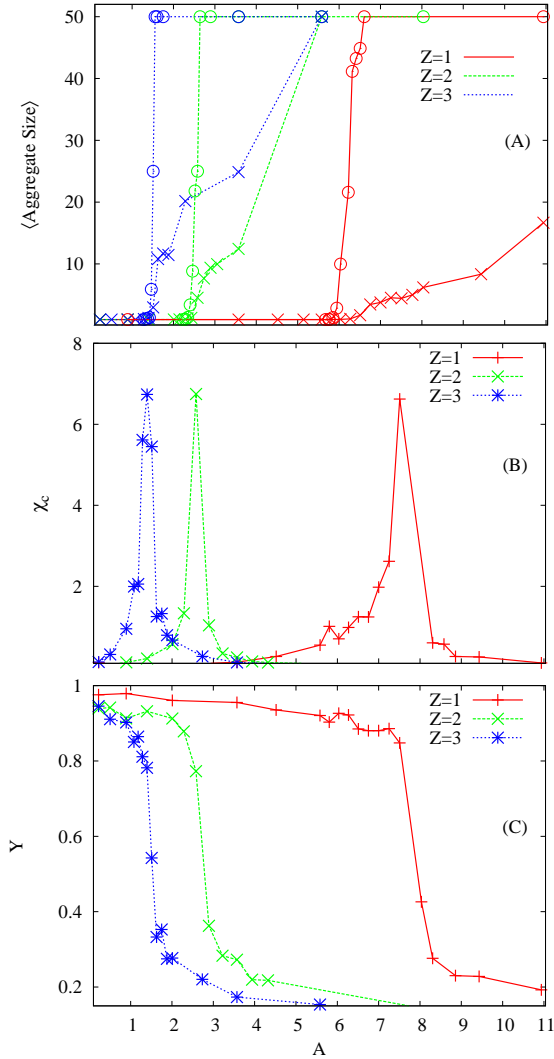
FIG. 2. (A) The variation of the average aggregate size with A. The data shown by crosses are obtained from simulations where the RLPEs are initially randomly distributed. For the data shown by circles we start at high value of A where initially all RLPEs are part of a single aggregate. The initial configuration for a lower value of A is the final configuration of the previous value of A. (B) The relative fluctuation χ_c in electrostatic energy of a single flexible PE as defined in Eq. (7). The height of the peaks have been rescaled for clarity. (C) The variation of asphericity Y [see Eq. (8)] with A of a single flexible PE chain.

the critical values, the aggregation kinetics is independent of A and the valency of the counterions. In Fig. 3, we show the time evolution of the history averaged number of aggregates $\langle N_a \rangle$. At the start of the simulations, the PEs are randomly distributed ($\langle N_a \rangle = 50$). After initial transients, corresponding to counterion condensation, $\langle N_a \rangle$ decays as a power law $t^{-\tau}$, with $\tau \approx 0.66$, independent of valency. If we model aggregation as irreversible coalescence of point-sized particles (see Ref.[54,55] for a review), then the above power law decay corre-
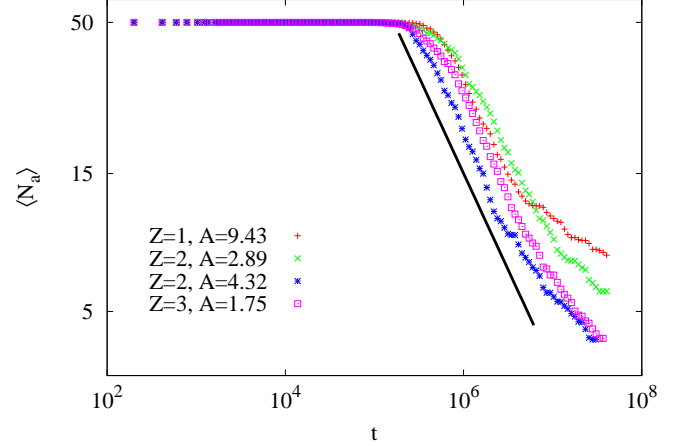
sponds to the diffusion constant of an aggregate of size m being proportional to $m^{-1/2}$.

In the earlier simulations[26–31], the interaction between similarly charged RLPEs in the presence of monovalent counterions was found to be repulsive. Typical values of A used in these simulations are 2.10^{26}, $2.90^{27,29}$ and 4.17^{28}, which are much smaller than the critical value (≈ 6.57) above which we observe the aggregate formation. We suggest that the absence of attractive interactions required for aggregation in these simulations can be attributed to the inappropriate values of A.

B. Extended-Collapsed transition of a single flexible polyelectrolyte chain

In our earlier simulations[44,45], we had demonstrated that a single flexible PE chain undergoes a first-order transition from an extended to a collapsed configuration, mediated by the counterions, when the parameter A exceeds a certain critical value. To establish a possible relation between the aggregation phenomena of RLPE chains and the extended–collapsed transition of a single flexible PE chain, we study the extended–collapsed transition of a single flexible PE chain of 600 monomers in the presence of monovalent and multivalent counterions. The density of the system is chosen as 2.7×10^{-6} monomers/σ^3 such that the direct contact between the PE chain and it's periodic images is avoided. The initial configuration of the PE chain is randomly chosen and the counterions are uniformly distributed inside the simulation box. The system is allowed to equilibrate for 10^7 steps and the averages are taken over a production run of 10^7 steps.

A useful quantity to study the extended–collapsed transition is the electrostatic energy per monomer E_c.

E_c shows different scaling with the number of monomers in the extended and collapsed phases[44]. The relative fluctuation χ_c in E_c is defined as

$$\chi_c = \frac{N \left[\langle E_c^2 \rangle - \langle E_c \rangle^2 \right]}{\langle E_c \rangle^2}. \tag{7}$$

Fig. 2(B) shows the variation of χ_c with A. χ_c has a peak around $7.5, 2.57$ and 1.40 for monovalent, divalent and trivalent counterions respectively. These peaks correspond to the extended–collapsed transition of the single PE chain.

The extended–collapsed transition can be further quantified by studying the variation of asphericity of the PE chain as a function of A. We define asphericity as

$$Y = \left\langle \frac{\lambda_1 - \frac{\lambda_2 + \lambda_3}{2}}{\lambda_1 + \lambda_2 + \lambda_3} \right\rangle, \tag{8}$$

where $\lambda_{1,2,3}$ are the eigenvalues of the moment of inertia tensor with λ_1 being the largest eigenvalue. The moment of inertia tensor G is

$$G_{\alpha\beta} = \frac{1}{N} \sum_{i=1}^{N} r_{i\alpha} r_{i\beta}, \tag{9}$$

where $r_{i\alpha}$ is the αth component of the position vector $\vec{r}_i$. Asphericity Y is zero for a sphere (collapsed globule) and one for a linear rod (extended configuration). For all other configurations, it has a value between zero and one.

The variation of Y with A is shown in Fig. 2(C). For all the three valencies, Y makes a transition from a value close to one (extended configuration) to zero (collapsed configuration) at a critical value of A. The transition in Y occurs at the same critical value of A where χ_c has a peak, and corresponds to the extended–collapsed transition of the PE chain. We note that these critical values roughly coincide with the critical values for the aggregation of RLPE chains in the presence counterions of the corresponding valency. This suggests the possibility that the underlying mechanisms of the collapse of a single PE chain and the aggregation of RLPE chains are closely related.

C. The effective interaction potential between two rod-like PE chains with monovalent counterions

To understand the observed aggregation of RLPEs in the presence of monovalent counterions, we measure the effective interaction potential between two similarly charged RLPEs. The effective interaction potential, for a separation d between the rods, is equal to the reversible work $W(d)$ done in bringing them from infinite separation to a separation of d. Since the system is overall charge neutral, we expect the interaction potential to be
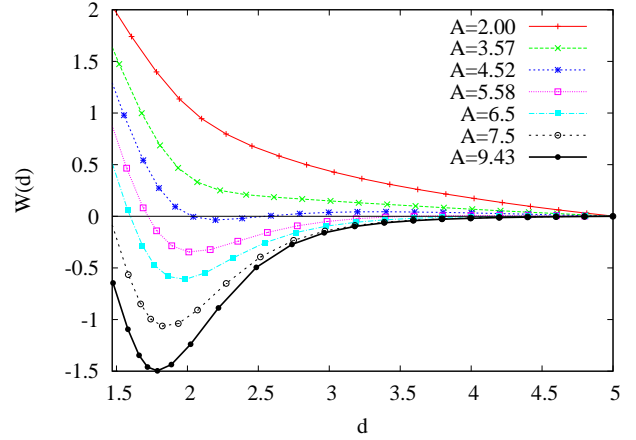

FIG. 4. The reversible work W needed to bring two rod-like PEs from a separation of 5σ to d, in the presence of monovalent counterions. The averages are taken over a production run of 10^7 steps, after the system has been equilibrated over 10^7 steps.

short-ranged, and hence $W(d)$ can be approximated by the work done in bringing the rods to a separation d from a finite separation d', where $d' > d$. $W(d)$ is then $\int_{d'}^{d} dx f(x)$, where $f(x)$ is the normal component of the force required to keep the two rods at a separation x.

For the evaluation of $W(d)$, we consider two parallel RLPEs of 30 monomers each. The system is charge neutralized by monovalent counterions. The density of the system is chosen to be 4.4×10^{-4} monomers/σ^3. Fig. 4 shows the variation of $W(d)$ per monomer for different values of A. For low values of A, $W(d)$ is always positive and decreasing with d, showing repulsion between the rods. At high values of A, $W(d)$ develops a minimum which is the onset of attraction between the rods. When the depth of the potential s comparable to thermal energy T, the attraction will be strong enough to form stable aggregates.

A similar evaluation of $W(d)$ for two similarly PEs in the presence of monovalent counterions was carried out in earlier simulations[29,30]. These simulations were performed at a range of values of A which is much less than the values at which we observe the attractive part in $W(d)$, and these simulations failed to observe the attractive part in $W(d)$. In Ref.[17], solving a simple model of PE system with monovalent counterions, the free energy was evaluated as a function of the separation between the rods. For the value of A studied ($A = 4.10$), it was shown that the depth of the attractive well was insufficient to bind the two PEs.

D. The angular distribution of the condensed counterions

It has been observed in experiments[56] and simulations[57] that the angular distribution of the condensed multivalent counterions changes as the PEs approach each other. Many theoretical studies[17,36,38] also argue that the spatial arrangement of the condensed multivalent counterions around the PEs plays an important role in developing an attractive interaction between the PEs.

We study the relationship between spatial distribution of counterion and the effective interaction between the RLPEs when all counterions are monovalent. For this, we consider the same system specifications as in Sec. III C. A counterion is said to have condensed on a PE if its separation from any of the monomers of the PE is less than 1.25σ. When the PEs come close by, the counterion may be shared by both the PEs, but the qualitative nature of the angular distribution remains the same. In Fig. 5, we show the dependence of $P(\theta)$ on θ, where $P(\theta)d\theta$ is the probability that the condensed counterion is between angle θ and $\theta + d\theta$. The data shown are for $A = 9.43$, for which a pronounced minimum in $W(d)$ was observed (see Fig. 4). Here, $\theta = 0$ or 2π corresponds to a location in the same plane and in between the two PEs, while $\theta = \pi$ corresponds to the counterion being located in the same plane but away away from the second PE. When the separation d between the PEs is much larger than 1.85σ, the condensed counterions are distributed uniformly around the PE. As the PEs approach each other, the distribution develops a sharp peak at $\theta = 0$, and a broad peak at $\theta = \pi$, showing that most condensed counterions are located in the same plane as that of the PEs, and mostly between the PEs. For separations less than 1.85σ, the peak at $\theta = 0$ is shifted to higher values, showing that the condensed counterions are expelled out of the plane of the two PEs, though they remain in the region between the PEs. This result is in accordance with Manning's theory[18] of shared counterions being the origin of attraction between two similarly charged PEs. The exclusion of counterions unscreens the interaction between the similarly charged monomers of the two PEs, causing the repulsion between them. These observations are consistent with the nature of the effective interaction potential between the PEs, i.e., attraction for intermediate separation($1.85\sigma \lesssim d \lesssim 4\sigma$) and repulsion at very small separation ($d \lesssim 1.85\sigma$).

IV. CONCLUSIONS

We studied, using molecular dynamics simulations, the role of the valency of the counterions on the aggregation of similarly charged RLPE chains. We showed that monovalent counterions can mediate the aggregation, provided the linear charge density of the PE backbone is larger than a critical value. The absence of aggregation in the presence of monovalent counterions in
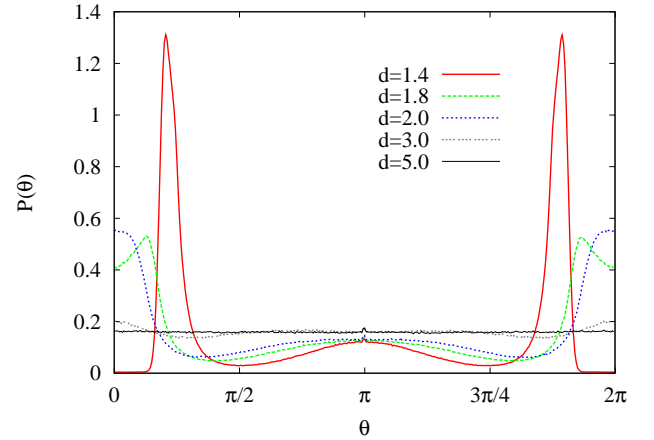

FIG. 5. The angular distribution $P(\theta)$ of condensed monovalent counterions around a given PE for $A = 9.43$.

earlier simulations and experiments is probably due to the linear charge density being smaller than the critical value. The critical linear charge density for aggregation decreases with increasing counterion valency, and is found to be close to the critical value for the extended–collapsed transition of a single flexible PE chain. We also find that, for two parallel RLPEs, the angular distribution of the condensed counterions changes with the separation between the chains. When the effective interactions are attractive, we find that the condensed counterions are shared by the RLPEs, similar to the mechanism suggested by Manning[18].

It would be interesting to study the aggregation transition in more detail. From our simulations, it appears that the phase transition is first-order in nature. However, using molecular dynamics simulations, it is difficult to equilibrate the system in the aggregating regime, especially if the initial density is low. Hybrid simulations using both Monte Carlo and molecular dynamics might be useful to study the transition[32,35].

Another problem of interest is the kinetics of aggregation. From our simulations, it appears that the density decay is independent of A and valency of the counterions. This may be due to fact that the attraction between two RLPEs is short-ranged for all values of A and valency. When two aggregates come close by, the probability that they aggregate may depend on A and valency. This, while affecting the prefactor of the power law decay, does not affect the exponent, suggesting that the kinetics is diffusion limited. Understanding the kinetics better, and also its dependence on hydrodynamic interactions will be part of a future study.

We note that the critical linear charge density for aggregation of RLPEs in the presence of monovalent counterions is much higher than that in the presence of multivalent counterions. One system which has comparable high linear charge densities is solutions of charged worm-like micelles[58,59]. Earlier Monte Carlo simulations of such

systems have used high charge densities[60]. Monovalent counterion induced aggregation, as seen in the current paper, may be realized in such charged micellar systems.

ACKNOWLEDGMENTS

REFERENCES

[1] A. V. Dobrynin and M. Rubinstein, Prog. Polym. Sci. **30**, 1049 (2005).

[2] R. R. Netz and D. Andelman, "Encyclopedia of electrochemistry," (Wiley-VCH, Weinheim, 2002) p. 282.

[3] Y. Levin, Rep. Prog. Phys. **65**, 1577 (2002).

[4] V. A. Bloomfield, Biopolymers **31**, 1471 (1991).

[5] J. X. Tang, S. Wong, P. T. Tran, and P. A. Janmey, Ber. Bunsenges. Phys. Chem. **100**, 796 (1996).

[6] M. Sedlák and E. J. Amis, J. Chem. Phys. **96**, 817 (1992).

[7] J. J. Tanahatoe and M. E. Kuil, J. Phys. Chem. B **101**, 5905 (1997).

[8] R. Borsali, H. Nguyen, and R. Pecora, Macromolecules **31**, 1548 (1998).

[9] B. D. Ermi and E. J. Amis, Macromolecules **31**, 7378 (1998).

[10] Y. Zhang, J. F. Douglas, B. D. Ermi, and E. J. Amis, J. Chem. Phys. **114**, 3299 (2001).

[11] O. V. Zribi, H. Kyung, R. Golestanian, T. B. Liverpool, and G. C. L. Wong, Phys. Rev. E **73**, 031911 (2006).

[12] F. Bordi, C. Cametti, M. Diociaiuti, and S. Sennato, Phys. Rev. E **71**, 050401(R) (2005).

[13] J. C. Butler, T. Angelini, J. X. Tang, and G. C. L. Wong, Phys. Rev. Lett. **91**, 028301 (2003).

[14] B. Y. Ha and A. J. Liu, Phys. Rev. E **60**, 803 (1999).

[15] B. Y. Ha and A. J. Liu, Physica A **259**, 235 (1998).

[16] B. Y. Ha and A. J. Liu, Phys. Rev. Lett. **79**, 1289 (1997).

[17] F. J. Solis and M. O. de la Cruz, Phys. Rev. E **60**, 4496 (1999).

[18] J. O. Ray and G. S. Manning, Macromolecules **33**, 2901 (2000).

[19] B. I. Skhlovskii, Phys. Rev. Lett. **82**, 3268 (1999).

[20] I. I. Potemkin, R. E. Limberger, A. N. Kudlay, and A. R. Khokhlov, Phys. Rev. E **66**, 011802 (2002).

[21] R. Bruinsma, Phys. Rev. E **63**, 061705 (2001).

[22] A. V. Ermoshkin and M. O. de la Cruz, Phys. Rev. Lett. **90**, 125504 (2003).

[23] S. Pietronave, L. Arcesi, C. D'Arrigo, and A. Perico, J. Phys. Chem. B **112**, 15991 (2008).

[24] A. Perico and A. Rapallo, J. Chem. Phys. **134**, 055108 (2011).

[25] G. S. Manning, Eur. Phys. J. E **34**, 132 (2011).

[26] N. G. Jensen, R. J. Mashl, R. F. Bruinsma, and W. M. Gelbart, Phys. Rev. Lett. **78**, 2477 (1997).

[27] M. J. Stevens, Phys. Rev. Lett. **82**, 101 (1999).

[28] A. Diehl, H. A. Carmona, and Y. Levin, Phys. Rev. E **64**, 011804 (2001).

[29] K. C. Lee, I. Borukhov, W. M. Gelbart, A. J. Liu, and M. J. Stevens, Phys. Rev. Lett. **93**, 128101 (2004).

[30] E. Allahyarov, G. Gompper, and H. Löwen, Phys. Rev. E **69**, 041904 (2004).

[31] A. Savelyev and G. A. Papoian, J. Am. Che. Soc. **129**, 660 (2007).

[32] M. Sayar and C. Holm, Euro. Phys. Lett. **77**, 10601 (2007).

[33] H. Fazli and R. Golestanian, Phys. Rev. E **76**, 041801 (2007).

[34] B. Luan and A. Aksimentiev, J. Am. Chem. Soc. **130**, 15754 (2008).

[35] M. Sayar and C. Holm, Phys. Rev. E **82**, 031901 (2010).

[36] J. J. Arenzon, J. F. Stilck, and Y. Levin, Eur. Phys. J. B **12**, 79 (1999).

[37] J. J. Arenzon, Y. Levin, and J. F. Stilck, Physica A **283**, 1 (2000).

[38] Y. Levin, J. J. Arenzon, and J. F. Stilck, Phys. Rev. Lett. **83**, 2680 (1999).

[39] G. S. Manning, Q. Rev. Biophys. **11**, 179 (1978).

[40] J. M. Shurr and B. S. Fujimoto, J. Phys. Chem. B **107**, 4451 (2003).

[41] R. Winkler, M. Gold, and P. Reineker, Phys. Rev. Lett. **80**, 3731 (1998).

[42] N. V. Brilliantov, D. V. Kuznetsov, and R. Klein, Phys. Rev. Lett. **81**, 1433 (1998).

[43] F. J. Solis and M. O. de la Cruz, J. Chem. Phys. **112**, 2030 (2000).

[44] A. Varghese, S. Vemparala, and R. Rajesh, J. Chem. Phys. **135**, 154902 (2011).

[45] A. Varghese, S. Vemparala, and R. Rajesh, AIP Conf. Proc. **1447**, 129 (2012).

[46] K. Jayasree, P. Ranjith, M. Rao, and P. B. S. Kumar, J. Chem. Phys. **130**, 094901 (2009).

[47] R. Golestanian, M. Kardar, and T. B. Liverpool, Phys. Rev. Lett. **82**, 4456 (1999).

[48] W. B. Russel, D. A. Saville, and W. R. Schowalter, *Colloidal Dispersions* (Cambridge University Press, Cambridge, 1989).

[49] See http://lammps.sandia.gov for details about the package.

[50] S. J. Plimpton, J. Comp. Phys. **117**, 1 (1995).

[51] S. Nosé, J. Chem. Phys **51**, 511 (1984).

[52] W. G. Hoover, Phys. Rev. A **31**, 1695 (1985).

[53] R. W. Hockney and J. W. Eastwood, *Computer Simulations Using Particles* (McGraw-Hill, New York, 1975).

[54] F. Leyvraz, Physics Reports **383**, 95 (2003).

[55] C. Connaughton, R. Rajesh, and O. Zaboronski, in *Handbook of Nanophysics: Clusters and Fullerenes*, edited by K. D. Sattler (Taylor and Francis, 2010).

[56] T. E. Angelini, H. Liang, W. Wriggers, and G. C. L. Wong, Eur. Phys. J. E **16**, 389 (2005).

[57] M. Deserno, A. Arnold, and C. Holm, Macromolecules **36**, 249 (2003).

[58] G. Jerke, J. S. Pedersen, S. U. Egelhaaf, and P. Schurtenberger, Langmuir **14**, 6013 (1998).

[59] C. Sommer, L. Cannavacciuolo, S. Egelhaaf, J. Pedersen, and P. Schurtenberger, in *Trends in Colloid and Interface Science XIV*, Progress in Colloid and Polymer Science, Vol. 115, edited by V. Buckin (Springer Berlin Heidelberg, 2000) pp. 347–352.

[60] L. Cannavacciuolo, J. S. Pedersen, and P. Schurtenberger, Langmuir **18**, 2922 (2002).